Journal of Optics

ACCEPTED MANUSCRIPT

Tunable polarization-sensitive optical nanoswitches based on spheroidal core-shell nanoparticles

To cite this article before publication: Ershad Mohammadi *et al* 2018 *J. Opt.* in press https://doi.org/10.1088/2040-8986/aad31b

Manuscript version: Accepted Manuscript

Accepted Manuscript is "the version of the article accepted for publication including all changes made as a result of the peer review process, and which may also include the addition to the article by IOP Publishing of a header, an article ID, a cover sheet and/or an 'Accepted Manuscript' watermark, but excluding any other editing, typesetting or other changes made by IOP Publishing and/or its licensors"

This Accepted Manuscript is **© 2018 IOP Publishing Ltd**.

During the embargo period (the 12 month period from the publication of the Version of Record of this article), the Accepted Manuscript is fully protected by copyright and cannot be reused or reposted elsewhere.
As the Version of Record of this article is going to be / has been published on a subscription basis, this Accepted Manuscript is available for reuse under a CC BY-NC-ND 3.0 licence after the 12 month embargo period.

After the embargo period, everyone is permitted to use copy and redistribute this article for non-commercial purposes only, provided that they adhere to all the terms of the licence https://creativecommons.org/licences/by-nc-nd/3.0

Although reasonable endeavours have been taken to obtain all necessary permissions from third parties to include their copyrighted content within this article, their full citation and copyright line may not be present in this Accepted Manuscript version. Before using any content from this article, please refer to the Version of Record on IOPscience once published for full citation and copyright details, as permissions will likely be required. All third party content is fully copyright protected, unless specifically stated otherwise in the figure caption in the Version of Record.

View the article online for updates and enhancements.

This content was downloaded from IP address 130.64.11.153 on 12/07/2018 at 20:57

Tunable Polarization-Sensitive Optical Nanoswitches Based On Spheroidal Core-Shell Nanoparticles

E. Mohammadi,[1,2*], F. A .Namin,[1] K. L. Tsakmakidis[3], F. Sohrabi[2,4],P. Dehkhoda[1], A. Tavakoli[1]

[1]*Department of Electrical Engineering, Amirkabir University of Technology, Tehran, Iran*

[2]*Bioengineering Department, École Polytechnique Fédérale de Lausanne (EPFL), Lausanne, Switzerland*

[3]*Department of Solid State Physics, National and Kapodistrian University of Athens, Athens, Greece*

[4]*Magneto-plasmonic Lab, Laser and Plasma Research Institute, Shahid Beheshti University, Tehran, Iran*

[*]Corresponding author: Email: ershad.mohammadi@epfl.ch

Abstract

In this paper we suggest the design of wavelength tunable, polarization-sensitive optical nanoswitches based on plasmonic spheroidal core-shell nanoparticles. Using a quasi-static approximation, we derive closed-form expressions for short and open circuit conditions, which respectively, provide extremely high and low permittivity values at optical frequencies. Owing to the anisotropic nature of spheroidal particles, the analysis are performed in longitudinal and transversal polarizations, where the electric field of impinging wave is along the major and minor axis of spheroid respectively. The derived formulas elucidate analytically this anisotropy, which has been implied by different short and open circuit conditions for two states of polarization. Our results show that by exploiting eccentricity in spheroidal core-shells (*i.e.*, compared to the spherical core-shells), the switching conditions can be transferred to infrared (IR) and ultraviolet (UV) frequencies, in longitudinal and transversal polarizations respectively. Finally, the effective permittivity of core-shell is extracted analytically using the concept of internal homogenization which gains insight into the optical response of particle. Our analysis pave the way toward realizing tunable and polarization dependent components in UV, optical and IR frequencies for sensing and nanocircuitry applications.

Keywords. plasmonics, spheroidal core-shell, optical nanoswitch, quasi-static

Accepted Manuscript

I. Introduction

In recent years there has been immense interest in the extension of circuit elements to optical wavelengths to design realistic nanocircuits [1–5]. Certain noble metals such as gold (Au), and silver (Ag) behave as plasmonic materials at the visible and near-IR range [6] and as a result these metallic nanoparticles display localized surface plasmon resonance [7]. Lumped circuit elements based on plasmonic nanoparticles were first introduced by Engheta et al.[1, 3]. Recent theoretical studies have demonstrated the possibility of designing more complex nanocircuit elements such as nanoswitches [8–10] and nanofilters [11–13] based on plasmonic nanoparticles.

Optical nanoswitches are an essential component of nanocircuits. Short and open circuit state of a switch correspond to perfect electric conductor (PEC) and perfect magnetic conductor (PMC) respectively, which are highly necessary but challenging to realize in optical frequencies. In [8] a nanoswitch composed of two conjoined hemispheres was proposed. Using quasi-static analysis, it was shown that near to the internal resonant frequency, the nanoparticle is highly anisotropic. For electric field polarized parallel to the interface of two hemispheres the particle was in the open-circuit state (corresponding to zero permittivity or PMC) and for electric field normal to the interface of two hemispheres, the nanoswitch was in the short-circuit state (corresponding to infinite permittivity or PEC).

In [10] a spherical core-shell structure was used to function as a nanoswitch. Using quasi-static approximation, conditions for the particle to exhibit either zero input admittance (open circuit), or zero input impedance (short circuit) were derived. It was shown that short- and open-circuit conditions occur at different wavelengths that can be tuned as desired by appropriately selecting the particles material constitution and geometrical characteristics such as volume fraction of core-shell (*i.e*. core's volume to the whole volume of particle).

In this paper we exploit spheroidal core-shell geometry to realize nanoswitches offering both anisotropy and tunability. These two features, respectively are fulfilled by exploiting spheroidal geometry and proper selection of volume fraction as well as material constitution. In addition, we demonstrate that the eccentricity of spheroidal core-shell as an emerging parameter, not only can increases the controlling features of switching, but it is capable of shifting the operating frequency of nanoswitch toward UV and IR frequencies. This ability of tuning working regime, offers unique implications for various sensing disciplines, in optical [14–16] and IR [17–19] as well as in UV range [20].

This paper is thus organized as follows: in section. II we perform quasi-static analysis both in longitudinal and transversal polarizations and derive the closed-form expressions for short and open circuit performance in each polarization. Then we derive the effective permittivity of core-shell based on internal homogenization concept [21] and re-derive the short and open circuit conditions based on this effective permittivity. In all analytical calculations the asymptotic approximations associated with spherical core-shell particles, are extracted and compared with previously reported

Accepted Manuscript

results [10]. Finally in section III, we discuss the analytical results and explore potential applications of our proposed nanoswitchs in metacircuits and sensing.

II. Theoretical Analysis

II. A. Prolate Spheroidal Core-Shell in Longitudinal Electric Field

A prolate spheroid is obtained by rotating an ellipse around its major axis. It is customary to make the z-axis the axis of revolution. The electromagnetic response of a prolate spheroid is polarization dependent. We start by considering the case where the electric field of the incident radiation is polarized along the major axis of the spheroid as depicted in Fig. 1. The relative dielectric constant of the particle core and shell are denoted by ε_c and ε_s respectively, and it is assumed that the particle is surrounded in a loss-less dielectric medium with dielectric constant ε_M .The prolate spheroidal coordinate system (ξ, η, φ) are related to rectangular coordinates by transformation [22]:

$$x = \frac{d}{2}\left[\left(1-\eta^2\right)\left(\xi^2-1\right)\right]^{1/2}\cos\phi \tag{1}$$

$$y = \frac{d}{2}\left[\left(1-\eta^2\right)\left(\xi^2-1\right)\right]^{1/2}\sin\phi \tag{2}$$

$$z = \frac{d}{2}\eta\xi \tag{3}$$

with: $-1 \le \eta \le 1$, $1 \le \xi \le \infty$ and $0 \le \phi \le 2\pi$, where d denotes the interfocal distance. The surface ξ = constant > 1 is a prolate spheroid with major axis of length $a = d\xi$ and minor axis of length $b = d(\xi^2-1)^{1/2}$ [22]. The eccentricity e is defined via

$$e = \frac{\xi}{\sqrt{\xi^2-1}} > 1 \tag{4}$$

For the geometry in Fig. 1 the volume fraction of the core, with respect to the volume of the core-shell particle, denoted by f is

Accepted Manuscript

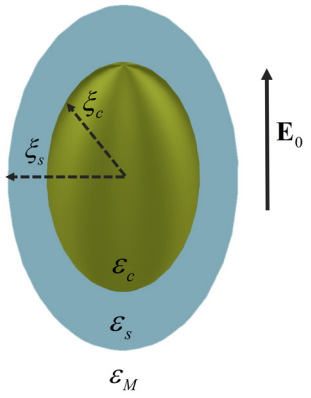

Fig. 1. Prolate spheroidal core-shell with impinging electric field along the major axis of particle (*i.e.*, longitudinal polarization).

$$f = \frac{\xi_c\left(\xi_c^{\,2}-1\right)}{\xi_s\left(\xi_s^{\,2}-1\right)} \tag{5}$$

For our analysis, we make the assumption that $b \ll \lambda_0$, where λ_0 is the wavelength of the incident wave. This assumption means that spatial field variations across the spheroid is negligible and thus we can analyze the problem using quasi-static approximation which requires solving the Laplace equation

$$\nabla^2\psi = 0 \tag{6}$$

To solve the Laplace equation in the prolate spheroidal coordinate system, we need the metrical coefficient h_η , h_ξ and h_ϕ which are defined by

$$h_x^2 + h_y^2 + h_z^2 = h_\eta^2 d_\eta^2 + h_\xi^2 d_\zeta^2 + h_\phi^2 d_\phi^2 \tag{7}$$

The scale factors h_η , h_ξ and h_ϕ in the prolate spheroidal coordinate system are [22]

$$h_\eta = \frac{d}{2}\left(\frac{\xi^2-\eta^2}{1-\eta^2}\right)^{1/2} \tag{8}$$

$$h_\xi = \frac{d}{2}\left(\frac{\xi^2-\eta^2}{\xi^2-1}\right)^{1/2} \tag{9}$$

$$h_\phi = \frac{d}{2}\left[\left(1-\eta^2\right)\left(\xi^2-1\right)\right]^{1/2} \tag{10}$$

The derivation of the solution to the Laplace equation for the prolate spheroidal core-shell gives the electrostatic ψ outside the core-shell as

$$\psi = \frac{-E_0 d}{2}\left[\xi + \frac{N}{D}Q_1(\xi)\right]\eta \tag{11}$$

where

$$N = \left(\varepsilon_s - \varepsilon_M\right)\xi_s\left[\varepsilon_s\xi_c Q_1'(\xi_c) - \varepsilon_c Q_1(\xi_c)\right] + \left(\varepsilon_c - \varepsilon_s\right)\xi_c\left[\varepsilon_s\xi_s Q_1'(\xi_s) - \varepsilon_M Q_1(\xi_s)\right] \tag{12}$$

Accepted Manuscript

$$D=\left(\varepsilon_M-\varepsilon_s\right)\left(\varepsilon_c-\varepsilon_s\right)\xi_c Q_1(\xi_s)Q_1'(\xi_s)+\left[\varepsilon_M\xi_s Q_1'(\xi_s)-\varepsilon_s Q_1(\xi_s)\right]\left[\varepsilon_s\xi_c Q_1'(\xi_c)-\varepsilon_c Q_1(\xi_c)\right] \tag{13}$$

and $Q_1(\cdot)$ is the Legendre function of the second kind [23]. It is worth mentioning that the plasmonic resonance condition for core-shell is achieved when D approaches to zero [24]. Here we consider the necessary conditions for the particle to exhibit short and open circuit responses. These conditions were derived in Ref.[10]. Basically the short circuit response is equivalent to setting the tangential electric field on the surface equal to zero

$$E_\eta=\left(\frac{1}{h_\eta}\frac{\partial\psi}{\partial\eta}\right)_{\xi=\xi_s}=0 \;\Rightarrow\psi\left(\xi_1\right)=0 \tag{14}$$

Conversely, the open-circuit response is equivalent to setting the normal electric field on the surface equal to zero

$$E_\xi=\left(\frac{1}{h_\xi}\frac{\partial\psi}{\partial\xi}\right)_{\xi=\xi_s}=0 \;\Rightarrow\left(\frac{\partial\psi}{\partial\xi}\right)_{\xi=\xi_s}=0 \tag{15}$$

Eq. (14) and Eq. (15) correspond to Dirichlet and Neumann boundary conditions, respectively. Enforcing Eq. (14) in Eq. (11), we arrive at the short-circuit condition

$$\frac{\varepsilon_c-\varepsilon_s}{\varepsilon_s}=\frac{\frac{\xi_s}{1-\xi_c^2}}{\xi_s Q_1(\xi_c)-\xi_c Q_1(\xi_s)} \tag{16}$$

Similarly, enforcing Eq. (15) in Eq. (11), we arrive at the open-circuit condition

$$\frac{\varepsilon_c-\varepsilon_s}{\varepsilon_s}=\frac{\frac{1}{1-\xi_c^2}}{Q_1(\xi_c)-\xi_c Q_1'(\xi_s)} \tag{17}$$

The conditions derived in Eq. (16) and Eq. (17) can only be satisfied when ε_s and ε_c have different signs. In the limiting case when $\xi_s,\xi_c\to\infty$, our structure becomes a spherical core-shell. Using the large-argument approximations of $Q_1(\cdot)$ and $Q_1'(.)$, the volume fraction in Eq. (5) is reduced to $f=\left(d\xi_c/d\xi_s\right)^3$ which is in accordance with volume fraction of a spherical core-shell. Accordingly Eq. (16) and Eq. (17) are respectively reduced to

$$\varepsilon_c=\varepsilon_s\frac{1+2/f}{1-1/f} \tag{18}$$

and,

$$\varepsilon_c=\varepsilon_s\frac{1-1/f}{1+1/2f} \tag{19}$$

Accepted Manuscript

which were derived in Ref.[10]. To gain more insight into the consequence of short and open circuit conditions over the entire response of particle, we extract the effective permittivity of core-shell by the concept of internal homogenization [21]. Here, we utilize the Clausius-Mossotti relation for this homogenization scheme[25] which results in the effective permittivity in longitudinal polarization as

$$\varepsilon_e^L = \varepsilon_s \frac{1+\frac{\varepsilon_c-\varepsilon_s}{\varepsilon_s}\left[\xi_c Q_1'(\xi_s)-Q_1(\xi_c)\right]\left[1-\xi_c{}^2\right]}{1+\frac{\varepsilon_c-\varepsilon_s}{\varepsilon_s}\left[\frac{\xi_c}{\xi_s}Q_1(\xi_s)-Q_1(\xi_c)\right]\left[1-\xi_c{}^2\right]} \tag{20}$$

Similar to Eq. (16) and Eq. (17), by using the large argument approximations for Legendre functions, the effective permittivity of a spherical core-shell is obtained as

$$\varepsilon_e = \varepsilon_s \frac{1+2f\frac{\varepsilon_c-\varepsilon_s}{\varepsilon_c+2\varepsilon_s}}{1-2f\frac{\varepsilon_c-\varepsilon_s}{\varepsilon_c+2\varepsilon_s}} \tag{21}$$

Based on the fact that, short and open circuit conditions ideally correspond to infinite and zero permittivity, the analytical expressions in Eq. (16) and Eq. (17) can be re-derived by equating the denominator and numerator of Eq. (20) to zero and infinity respectively.

II. B. Prolate Spheroidal Core-Shell in Transversal Electric Field

In the previous section short and open circuit conditions are derived when the polarization of electric field was along the major axis. Duo to the anisotropic nature of spheroidal particles we expect different conditions for polarized electric field along the minor axis as illustrated in Fig. 2.

Accepted Manuscript

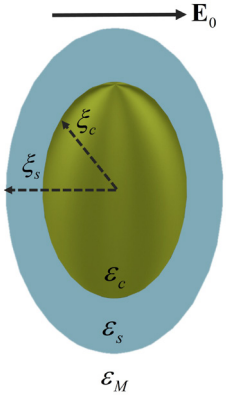

Fig. 2. Prolate spheroidal core-shell with impinging electric field along the minor axis of particle (*i.e.*, transversal polarization)

Solving the Laplace equation in (6) gives the solution to the electrostatic ψ outside the core-shell as

$$\psi = -\frac{E_0 d}{2}\left[\sqrt{\xi^2-1}+\frac{N}{D}Q_1^1(\xi)\right]\sqrt{1-\eta^2}\cos\phi \tag{22}$$

where,

$$N = \left(\varepsilon_s-\varepsilon_M\right)\xi_s\left[\frac{2\varepsilon_s}{1-\xi_c^{\,2}}+\frac{\left(\varepsilon_s-\varepsilon_c\right)\xi_c Q_1^1(\xi_c)}{\sqrt{\xi_c^{\,2}-1}}\right]+ \left(\varepsilon_c-\varepsilon_s\right)\xi_c\left[\frac{2\varepsilon_s}{1-\xi_s^{\,2}}+\frac{\left(\varepsilon_s-\varepsilon_M\right)\xi_s Q_1^1(\xi_s)}{\sqrt{\xi_s^{\,2}-1}}\right] \tag{23}$$

$$D = \left(\varepsilon_M-\varepsilon_s\right)\left(\varepsilon_c-\varepsilon_s\right)\xi_c Q_1^1(\xi_s)Q_1^{1\prime}(\xi_s)+ \left[\frac{2\varepsilon_M}{1-\xi_s^{\,2}}+\frac{\left(\varepsilon_M-\varepsilon_s\right)\xi_s Q_1^1(\xi_s)}{\sqrt{\xi_s^{\,2}-1}}\right]\left[\frac{2\varepsilon_s}{1-\xi_c^{\,2}}+\frac{\left(\varepsilon_s-\varepsilon_c\right)\xi_c Q_1^1(\xi_c)}{\sqrt{\xi_c^{\,2}-1}}\right] \tag{24}$$

and $Q_1^1(.)$ is the associated Legendre function of the second kind [23]. Enforcing Eq. (14) and (15) in Eq. (22), gives the short and open circuit conditions for transversal polarization as

$$\frac{\varepsilon_c-\varepsilon_s}{\varepsilon_s} = \frac{\dfrac{2}{\xi_c\left(1-\xi_c^{\,2}\right)}}{\dfrac{Q_1^1(\xi_s)}{\sqrt{\xi_s^{\,2}-1}}-\dfrac{Q_1^1(\xi_c)}{\sqrt{\xi_c^{\,2}-1}}} \tag{25}$$

Accepted Manuscript

$$\frac{\varepsilon_c-\varepsilon_s}{\varepsilon_s}=\frac{\frac{2}{\xi_c^{\,2}-1}}{\xi_c Q_1^{1\prime}(\xi_s)-\frac{\xi_c}{\sqrt{\xi_c^{\,2}-1}}Q_1^1(\xi_c)} \tag{26}$$

respectively. The conditions derived in Eq. (25) and Eq. (26), again can only be satisfied when core and shell permittivities are of different signs. It can be shown that under large argument approximation for $Q_1^1(.)$ and $Q_1^{1\prime}(.)$ the expressions in Eq. (25) and Eq. (26) are reduced to Eq. (18) and Eq. (19) respectively. Similar to Sec. II.A, here we extract the effective permittivity in transversal polarization as

$$\varepsilon_e^T=\varepsilon_s\frac{1+\frac{(\varepsilon_c-\varepsilon_s)\frac{\xi_c}{\xi_s}Q_1^{1\prime}(\xi_s)\sqrt{\xi_s^{\,2}-1}}{(\varepsilon_s-\varepsilon_c)\frac{\xi_c}{\sqrt{\xi_c^{\,2}-1}}Q_1^1(\xi_c)+\frac{2\varepsilon_s}{1-\xi_c^{\,2}}}}{1+\frac{(\varepsilon_c-\varepsilon_s)\frac{\xi_c}{\sqrt{\xi_s^{\,2}-1}}Q_1^1(\xi_s)}{(\varepsilon_s-\varepsilon_c)\frac{\xi_c}{\sqrt{\xi_c^{\,2}-1}}Q_1^1(\xi_c)+\frac{2\varepsilon_s}{1-\xi_c^{\,2}}}} \tag{27}$$

It can be seen that short and open circuit conditions in Eq. (25) and Eq. (26) are similar to the denominator and numerator of Eq. (27) and cab be re-extracted via effective permittivity approach as explained in Sec. II. A.

III. Discussion

To verify the validity of our results, we used the electrostatic solver of the software package, COMSOL Multiphysics. In the simulations, the radius of core and shell for spheroid particle are assumed to be 50 nm and 100 nm, respectively. In this case, the eccentricity of particle (either core or shell) is enforced by the interfocal distance which herein is taken as d = 90 nm. This value of interfocal distance leads to eccentricities of $e_c = 2.29$ and $e_s = 1.12$ for core and shell respectively. For the shell permittivity we consider a typical value of $\varepsilon_s = 6.75$.

Fig. 3 shows the simulation results across a cut-plane of spheroidal core-shell when the impinging electric field is along the major axis of particle. By choosing aforementioned geometrical parameters for core-shell, the corresponding core permittivity values for short and open circuit performance in longitudinal polarization, are obtained as $\varepsilon_c^{sc} = -41.5$ and $\varepsilon_c^{oc} = -33$, via equation (16) and Eq. (17) respectively. In Fig.3a the electric potential distribution along with electric field lines (black streamlines) are shown for short circuit state where Eq. (16) is satisfied. The direction of displacement current flux, which is highlighted by yellow arrows, well clarify the entering and the

Accepted Manuscript

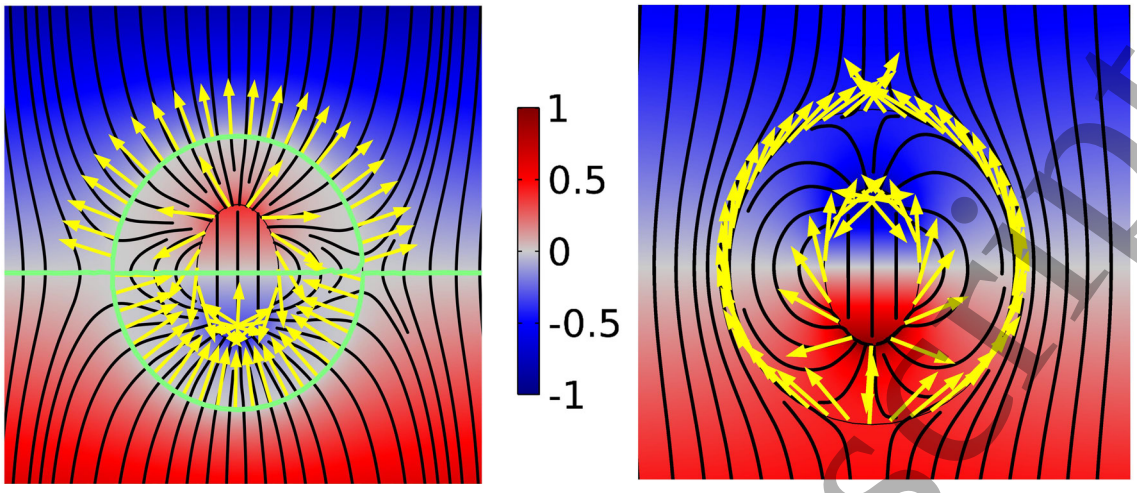

Fig. 3. Distribution of electric potential along with electric field lines (black streamlines), as well as displacement current flux (yellow arrows) for (a) Short and (b) open circuit states of a spheroidal core-shell nanoswitch placed in a longitudinal electric field as depicted in Fig.1. Geometrical parameters and material permittivities for core-shell, have been chosen such that Eq. (16) and Eq. (17) are satisfied respectively. The green contour in (a) shows the formation of zero potential in short circuit state.

exiting optical current over the down and top hemispheres of particle as two ports of nanoswitch component. The normal flow of this flux into the core-shell surface as well as the zero potential contour which encircled the particle (highlighted by green) demonstrate the short circuit performance of nanoswitch. Similarly in Fig. 3b the open-circuit performance of particle is ensured by fulfilling Eq. (17). As expected, in this case, the normal electric field on the outer surface of the spheroid goes to zero and thus, likewise to the open circuit state of a switch, the optical current can not enter to the component.

In Fig. 4 the same simulations were presented in Fig.3 have been performed, but this time for transversal polarization. In this case, by using the same parameters as in Fig. 3, the core permittivity values associated with short and open circuit conditions are attained as $\varepsilon_c^{sc} = -9.5$ and $\varepsilon_c^{oc} = -8.3$, via equation (25) and equation (26) respectively. In Fig. 4a and Fig. 4b, it can be seen that, again, in short circuit case the optical current flows normal to the particle and zero potential contour is also formed around the core-shell, while in the open circuit state the optical current is bypassed around the component. Analogous field distributions in short and open circuit states in Fig. 3 and Fig. 4 with electric field patterns around PEC and PMC objects, elucidate how these two states can provide extremely high and low permittivity values respectively.

In Fig.3 and Fig.4 we investigated the realization of short and open circuit states by assigning negative and positive dispersion-less permittivities to core and shell respectively. However in optical frequencies negative values of permittivity are commonly achieved by highly dispersive metals such as gold (Au) and silver (Ag). Utilizing these materials in nanoswitch component makes the response of particle to be dependent on wavelength. To explore the frequency response of so-attained components, we use a plasmonic gold core with Drude dispersion parameters of $\varepsilon_\infty = 9$, $\omega_p = 13.8e15$. Firstly we assume that both core and shell materials are lossless. Without loss of generality, this assumption makes it much easier to analytically characterize the short and open circuit wavelengths associated with derived permittivities in Eq. (16-17) and Eq. (25-26).

Accepted Manuscript

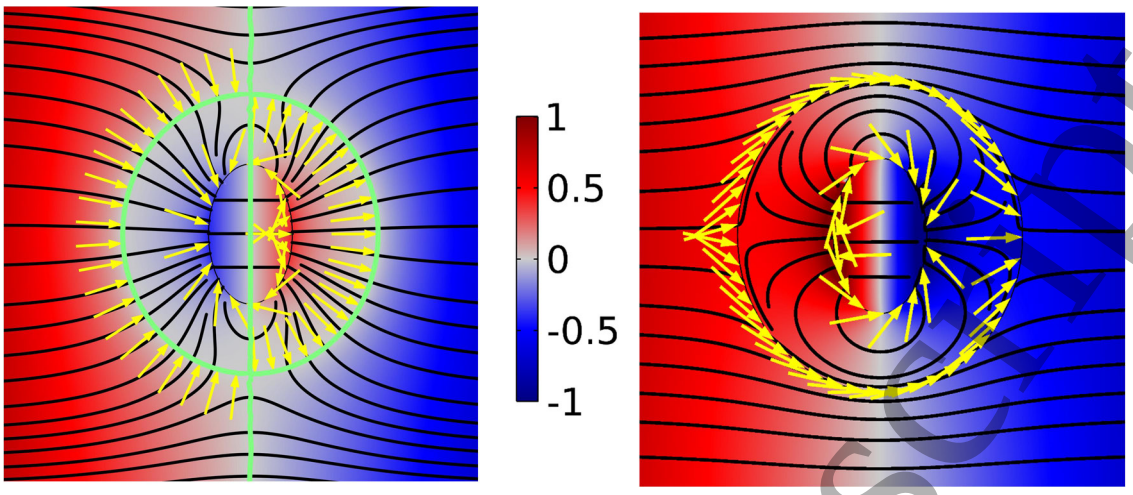

Fig. 4. Distribution of electric potential along with electric field lines (black streamlines), as well as displacement current flux (yellow arrows) for (a) Short and (b) open circuit states of a spheroidal core-shell nanoswitch placed in a transversal electric field as depicted in Fig.2. Geometrical parameters and material permittivities for core-shell, have been chosen such that Eq. (25) and Eq. (26) are satisfied respectively. The green contour in (a) shows the formation of zero potential in short circuit state.

Fig. 5 shows switching performance analysis as a function of wavelength and volume fraction as well as the material constitution for both spherical and spheroidal core-shell elements. The geometrical parameters for spheroidal core-shell are the same as the previous study in Fig. 3 and Fig.4. For comparative studies, the radius of core and shell in spherical particle, are chosen as 50 nm and 100 nm, which respectively are equal to the length of major semi-axes of core and shell in spheroidal one. For spherical particle, different volume fractions on vertical axis are achieved by increasing the core radius while keeping the shell radius constant at 100 nm. Likewise for spheroidal core-shell the major semi-axis of shell and the focal distance are kept constant at 100 nm and 90 nm respectively, and the major semi-axis of core is raised.

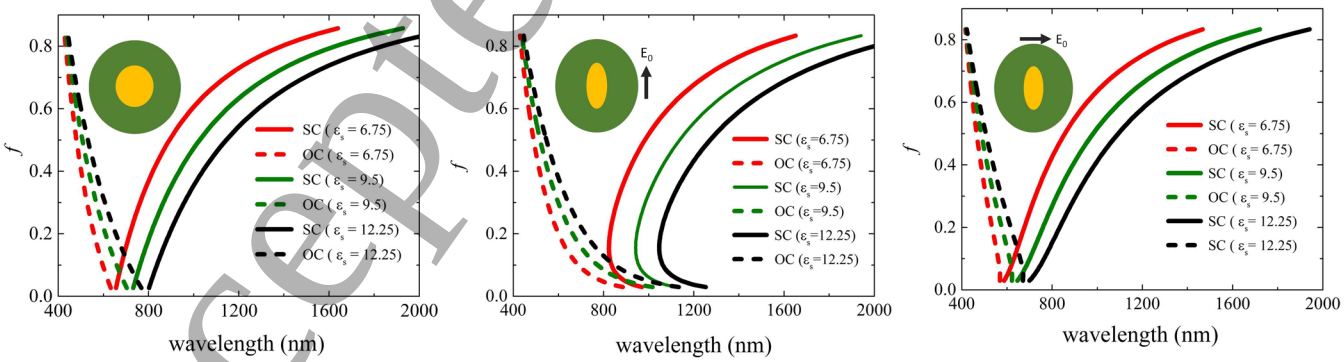

Fig. 5. Short and open circuit switching conditions as a function of operating wavelength and volume fraction as well as material constitution, corresponding to (a) Eq. (18-19) for spherical core-shell, (b) Eq. (16-17) for spheroidal core-shell in longitudinal electric field and (c) spheroidal core-shell in transversal electric field. In all analysis the core material is assumed as lossless gold while the shell is dielectric with changing permittivity.

It is evident from Fig. 5 that increasing the volume fraction in either spherical or spheroidal core-shells can shifts the short circuit condition toward IR frequencies. An explanation to this behavior is

Accepted Manuscript

that, at higher values of volume fraction the shell thickness is very small and the plasmonic core must provide the infinite effective permittivity individually, which is required for short circuit performance. Noting that the absolute value of gold negative permittivity gets larger by increasing in wavelength, this infinite permittivity can be offered at higher wavelengths. Oppositely, it can be seen that low volume fractions, transfers the OC condition form UV to optical frequencies which similarly can be explained. In fact, noting that in open circuit condition the effective permittivity approaches zero, it can be concluded that as the plasmonic core gets smaller, its effect must be enhanced to compensate the contribution of positive permittivity of shell. This enhanced effect is again provided at higher wavelengths.

According to the aforementioned explanations, it is clear that both spherical and spheroidal core-shells are common in their red and blue shift features for short and open circuit conditions with increasing volume fraction. However an interesting behavior which has not been explored before, is the ability of eccentricity to produce similar effects. According to Fig. 5b, it can be seen that switching conditions for spheroidal particle in longitudinal polarization, are transferred to IR frequencies even in small volume fractions, while for transversal polarization in Fig. 5c are shifted slightly toward UV wavelengths. In Fig. 6 we have investigated this effect more specifically by increasing the eccentricity and comparing the resulted switching conditions with spherical core-shell. We have selected geometric parameters as in Fig. 5, with the difference that, here the focal distance is changed for achieving higher values of eccentricity. Three studies in Fig. 6 are associated with focal distances of $d = 40\ \text{nm}, 45\ \text{nm}, 47\ \text{nm}$ corresponding to maximum core eccentricity (for lowest volume fraction) of e_c =1.67, 2.3, 2.93 respectively. It is well-evident from Fig. 6 that how higher values of eccentricity enhance the red and blue shifts in longitudinal and transversal switching conditions.

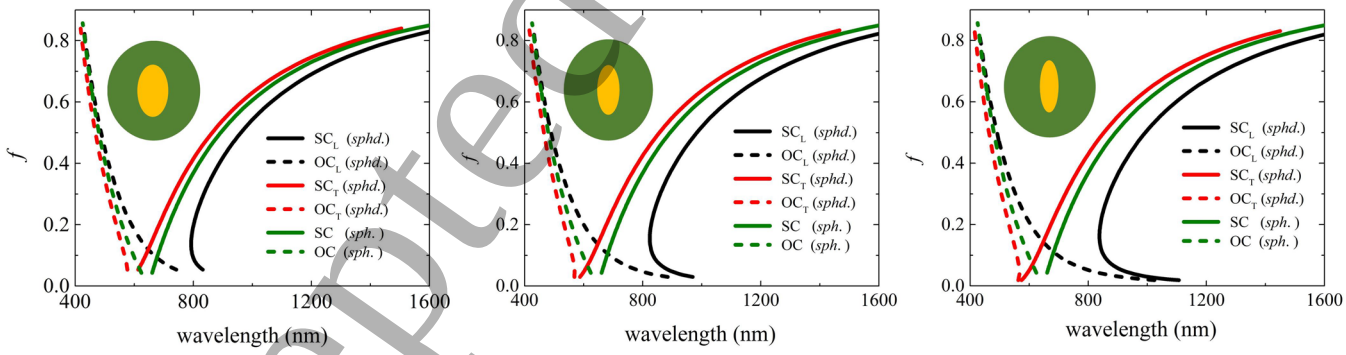

Fig. 6. Short and open circuit switching conditions as a function of operating wavelength and volume fraction as well as eccentricity. Three studies are associated with maximum core eccentricities of (a) e_c =1.67 (b) e_c =2.3 and (c) e_c =2.93. In all studies the core material is assumed as lossless gold while the shell is dielectric with permittivity of $\varepsilon_c = 6.75$.

In order to gain a better insight into the above mentioned property, in Fig. 7 we have plotted the effective permittivity as a function of wavelength and volume fraction. Here we additionally, included loss effects by adding the loss factor to the gold Drude model. Fig. 7a shows the effective permittivity for spherical core-shell derived in Eq. (21), while Fig. 7b and Fig. 7c illustrate the

Accepted Manuscript

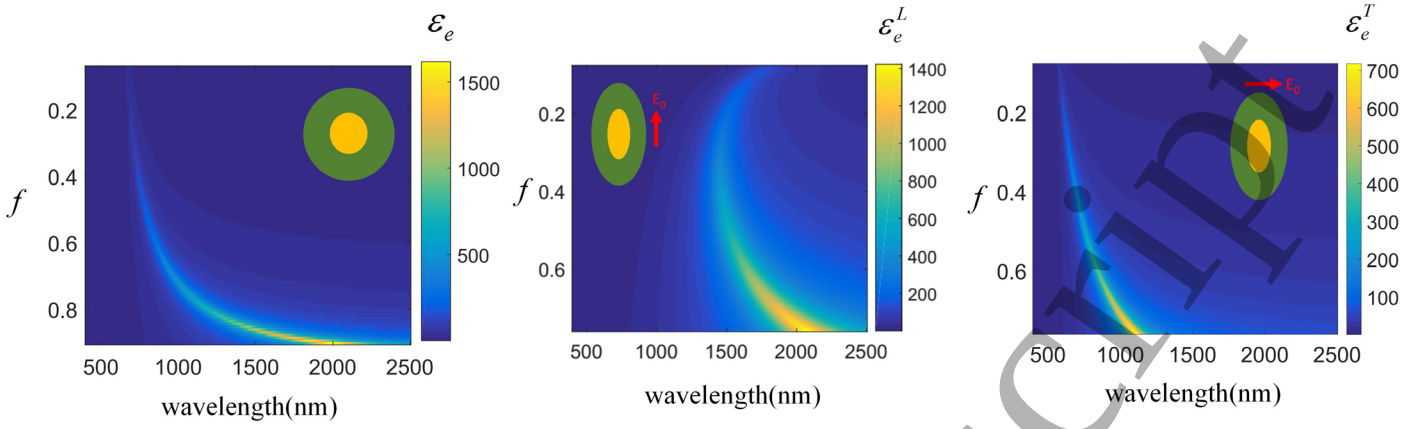

Fig. 7. The effective permittivity of (a) spherical, (b) spheroidal in longitudinal polarization and (c) spheroidal in transversal polarization, as a function wavelength and volume fraction. Three panels in (a)-(c) corresponds to Eq. (21), Eq. (20) and Eq. (27) respectively.

effective permittivity of spheroidal core-shell for longitudinal and transversal polarizations, which respectively derived in Eq. (20) and Eq. (27).The radius and major semi-axis of shell, associated with spherical and spheroidal particles are fixed both at 60 nm, and the core radius/major semi-axis is changed for archiving different volume fractions. The interfocal distance is considered as d = 50 nm which gives the shell eccentricity of e_s = 1.8 and the maximum core eccentricity of e_c = 5. The bright contours on plots indicate the short circuit condition realization, which corresponds to high values of effective permittivity. Approving previously obtained results, Fig. 7 clearly illustrates how the short circuit condition is shifted to the IR and UV frequencies in longitudinal and transversal polarizations respectively.

Conclusion

In this paper we introduced spheroidal core-shell particles, as a new category of optical nanoswitchs, offering simultaneously both anisotropy and tunability. We performed the quasi-static analysis of particle, in longitudinal and transversal polarizations which resulted the closed-form expressions for short and open circuit performance of particle in each polarization. The polarization dependency of spheroidal cores-shells which is implied by different analytical expressions for different polarizations, can provide anisotropic nanoswitchs with possible application in optical parallel processing. Additionally we studied the volume fraction and material constitution of core and shell as two tuning features of nanoswitch. Finally, we demonstrated how the eccentricity of spheroidal particles can shift the switching conditions toward IR or UV wavelengths.

Accepted Manuscript

References

1. Engheta N (2007) Circuits with light at nanoscales: optical nanocircuits inspired by metamaterials. Science (80-) 317:1698–1702
2. Alu A, Engheta N (2008) Tuning the scattering response of optical nanoantennas with nanocircuit loads. Nat Photonics 2:307
3. Engheta N, Salandrino A, Alù A (2005) Circuit elements at optical frequencies: nanoinductors, nanocapacitors, and nanoresistors. Phys Rev Lett 95:95504
4. Sun Y, Edwards B, Alù A, Engheta N (2012) Experimental realization of optical lumped nanocircuits at infrared wavelengths. Nat Mater 11:208
5. Shi J, Monticone F, Elias S, et al (2014) Modular assembly of optical nanocircuits. Nat Commun 5:3896
6. Cai W, Shalaev VM (2010) Optical metamaterials. Springer
7. Maier SA (2007) Plasmonics: fundamentals and applications. Springer Science & Business Media
8. Alù A, Engheta N (2009) Optical nanoswitch: an engineered plasmonic nanoparticle with extreme parameters and giant anisotropy. New J Phys 11:13026
9. Sadeghi SM (2010) Tunable nanoswitches based on nanoparticle meta-molecules. Nanotechnology 21:355501
10. Panaretos AH, Werner DH (2013) Tunable wavelength dependent nanoswitches enabled by simple plasmonic core-shell particles. Opt Express 21:26052–26068
11. Gil M, Bonache J, Martin F (2008) Metamaterial filters: A review. Metamaterials 2:186–197
12. Abbasi F, Engheta N (2014) Roles of epsilon-near-zero (ENZ) and mu-near-zero (MNZ) materials in optical metatronic circuit networks. Opt Express 22:25109–25119
13. Alù A, Young ME, Engheta N (2008) Design of nanofilters for optical nanocircuits. Phys Rev B 77:144107
14. Endo T, Kerman K, Nagatani N, et al (2006) Multiple label-free detection of antigen− antibody reaction using localized surface plasmon resonance-based core− shell structured nanoparticle layer nanochip. Anal Chem 78:6465–6475
15. Chung T, Lee S-Y, Song EY, et al (2011) Plasmonic nanostructures for nano-scale bio-sensing. Sensors 11:10907–10929
16. Mohammadi E, L. Tsakmakidis K, Askarpour A, et al (2018) Nanophotonic platforms for enhanced chiral sensing. ACS Photonics
17. Bontempi N, Vassalini I, Alessandri I (2018) All-dielectric core/shell resonators: From plasmon-free SERS to multimodal analysis. J Raman Spectrosc
18. Bontempi N, Vassalini I, Danesi S, Alessandri I (2017) ZORRO: zirconium oxide resonators for all-in-one Raman and whispering-gallery-mode optical sensing. Chem Commun 53:10382–10385
19. Adato R, Yanik AA, Amsden JJ, et al (2009) Ultra-sensitive vibrational spectroscopy of protein monolayers with plasmonic nanoantenna arrays. Proc Natl Acad Sci 106:19227–19232
20. Whitmore L, Wallace BA (2008) Protein secondary structure analyses from circular dichroism spectroscopy: methods and reference databases. Biopolym Orig Res Biomol 89:392–400
21. Chettiar UK, Engheta N (2012) Internal homogenization: Effective permittivity of a coated sphere. Opt Express 20:22976–22986
22. Flammer C (2014) Spheroidal wave functions. Courier Corporation
23. Arfken GB, Weber HJ, Harris FE (2011) Mathematical methods for physicists: a comprehensive guide. Academic press

Accepted Manuscript

24. Norton SJ, Vo-Dinh T (2007) Plasmon resonances of nanoshells of spheroidal shape. IEEE Trans Nanotechnol 6:627
25. Shalaev VM (1996) Electromagnetic properties of small-particle composites. Phys Rep 272:61–137

Accepted Manuscript